European Journal of Medicinal Chemistry 69 (2013) 223–231

Contents lists available at ScienceDirect

European Journal of Medicinal Chemistry

journal homepage: http://www.elsevier.com/locate/ejmech

Original article

Preparation and biological evaluation of ^{99m}Tc-N4IPA for single photon emission computerized tomography imaging of hypoxia in mouse tumor

Nan Li [a], Hua Zhu [a], Tai-wei Chu [b], Zhi Yang [a,*]

[a] Key Laboratory of Carcinogenesis and Translational Research (Ministry of Education), Department of Nuclear Medicine, Peking University Cancer Hospital & Institute, Beijing, China
[b] Beijing National Laboratory for Molecular Sciences, Radiochemistry and Radiation Chemistry Key Laboratory of Fundamental Science, College of Chemistry and Molecular Engineering, Peking University, Beijing 100871, China

ARTICLE INFO

Article history:
Received 22 March 2013
Received in revised form
9 July 2013
Accepted 2 August 2013
Available online 24 August 2013

Keywords:
Technium-99m
4-Nitroimidazoles
Hypoxia imaging
Tumor

ABSTRACT

In order to develop technetium-99m labeled nitroimidazole imaging agent for hypoxia in tumor, we have synthesized ^{99m}Tc-1-(4-nitroimidazole-yl)-propanhydroxyiminoamide, ^{99m}Tc-N4IPA complex, in high radiochemical purity and radiochemical yield. The biological evaluation of this complex includes the in vitro/vivo stability, cell uptake and Single Photon Emission Computerized Tomography (SPECT) imaging in mouse tumor models, respectively. These results demonstrate that ^{99m}Tc-N4IPA may have potential as clinical hypoxia imaging agent. The key features of the biological evaluation include the following: (1) the autoradiogram of ^{99m}Tc-N4IPA complex in tissue samples of hypoxia overlaps with the area stained by hypoxyprobe-1; (2) SPECT imaging of U87-bearing mice clearly identifies tumors 4 h post injection of ^{99m}Tc-N4IPA, reaching ID% of 8.48 ± 4.51; (3) the main pathways of excretion of ^{99m}Tc-N4IPA are through kidneys and livers in both A549 or U87-bearing tumor mice.

1. Introduction

Hypoxia is a common feature of solid tumors. It is strongly associated with tumor growth, proliferation, metastasis and resistance to therapy, and it has become a central issue in tumor physiology and cancer treatment [1,2]. Hypoxia in tumors plays an important role in resistance to radiotherapy and chemotherapy, it is important to assess tumor hypoxia to select proper treatment. Nuclear imaging provides a noninvasive method for its identification. A lot of efforts have been devoted to the development of radiolabeled imaging agents for tumor hypoxia. Radiolabeled derivatives of nitroimidazoles are one class of such agents [3,4]. Recently a number of ^{99m}Tc-labeled nitroimidazole-containing agents, based on 2-nitromidazole derivatives, for example, BMS181321 and BRU59-21, have been developed as imaging agents, but with high lipophilicity and slow blood clearance [5–7]. The chelators chosen for radiolabelling with ^{99m}Tc have been boronic acid adduct of technetium dioxime (BATO) or propylene amine oxime-containing (PnAO-containing) compounds. Those complex structures may affect the accuracy of hypoxic detection [8].We have designed and synthesized a number of ^{99m}Tc radiolabeled hydroxyiminoamide derivatives as SPECT imaging for tumor hypoxia [9–11], based on the following two main observations. A small number of studies have found that 4(5)-nitro-imidazole containing compounds can also accumulate in hypoxia cells [12,13]. Yang et al., developed 5-nitrimidazole derivatives to image tumor hypoxia [14], and ^{99m}Tc-N5IPA has showed good hypoxic selectivity both in cells and tumor in vitro/in vivo. Boronic acid adduct of technetium dioxime (BATO) or propylene amine oxime (PnAO) can serve as core structure of the chelating complex of technetium [15,16], and hydroxyiminoamides and ^{99m}Tc could form highly stable complexes both in vitro and in vivo [17]. Nakayama et al., found that hydroxyiminoamides could form highly in vivo and in vitro stable complexes with ^{99m}Tc and might be useful new chelating moiety for design ^{99m}Tc radiopharmaceuticals [18]. However, in their study the compounds were just limited to the compounds containing phenyl group. In this study, we report our work on the synthesis, and biological evaluation of ^{99m}Tc-1-(4-nitroimidazole-1-yl)-propanhydroxyiminoamide, ^{99m}Tc-N4IPA complex.

* Corresponding author. Department of Nuclear Medicine, Peking University School of Oncology, Beijing Cancer Hospital & Institute, Beijing 100142, China. Tel./fax: +86 10 8819 6196.
E-mail addresses: zhuhuananjing@163.com (H. Zhu), pekyz@163.com (Z. Yang).

0223-5234/$ – see front matter © 2013 Elsevier Masson SAS. All rights reserved.
http://dx.doi.org/10.1016/j.ejmech.2013.08.005

2. Materials and methods

3-Bromopropionitrile, 4-nitroimidazole, triethylamine, phosphate-buffered saline (PBS), sodium tartrate, hydroxylamine, and bovine serum albumin (BSA) were purchased from Sigma–Aldrich (St. Louis, MO, USA). Na[$^{99m}TcO_4$] was eluted from a $^{99}Mo/^{99m}Tc$ generator (China Isotope and Radiation Co. Ltd, Beijing, China) using saline. Other commercial materials were purchased from VWR International (San Diego, CA, USA). All reagents were analyzed before use. All synthesized chemicals were characterized by ^1H NMR. Melting points were determined on WRS-IA apparatus and were uncorrected.

Radiochemical purity was checked both with radioactivity thin-layer scanner (Bioscan, IAR-2000, Washington DC, USA), and HPLC (Agilent, USA), with Zorbax SB-C18 (4.6 mm × 250 mm, 5 μm) using gradient program as follows: 0–10 min: 0%–20%B; 10–15 min: 20%–90%B; 15–20 min: 90%–50%B; 20–21 min: 50%–10% B and the flow rate 1.0 mL/min. Solvent A was PBS (pH 6.0, 10 mM) and solvent B was CH_3CN. The radioactivity was measured using an automated gamma scintillation counter (Perkin Elmer, 1470-002, USA). Autoradiogram was captured using a high-sensitivity imaging film (BAS-SR2025, Fuji Photo Film, Japan), and scanned using computerized imaging analysis system (PLA5100, Fuji medical-system, USA, Stanford, CT). In vivo SPECT imaging was performed on a SPECT camera (Siemens, E cam, Germany).

Chinese hamster ovary (CHO) cell line was provided by the Department of Genetic Research, Beijing Cancer Hospital. Human glioma U87 and human lung cancer A549 cells were provided by the College of Life Sciences, Beijing University. Dulbecco's Modified Eagle's Medium (DMEM) was purchased from Gibco BRL Life Technologies (Grand Island, NY, USA) and fetal bovine serum, from Hyclone (Logan, UT, USA). The mice were kept under specific pathogen free conditions and were handled and maintained according to Institutional Animal Care and Use Committee guidelines.

2.1. Synthesis and radiolabeling of ^{99m}Tc-N4IPA

1-(4-Nitroimidazole-1-yl)-propanhydroxyiminoamide (N4IPA) was synthesized according to a reported procedure with some modification [10,15]. Briefly, 3-Bromopropionitrile (2.66 g, 20.0 mmol) was added to the suspension of 4-nitroimidazole (1.13 g, 10.0 mmol) in triethylamine (10 mL), and the mixture was refluxed in an oil-bath for 4 h. 1-(2-Cyanoethyl)-4-nitroimidazole (1.33 g, 8 mmol, yield 80%) was obtained as a white solid by recrystallization from methanol. m.p. 109–110 °C. ^1H NMR ($CDCl_3$, 500 MHz) δ: 3.17 (t, $J = 4.0$ Hz, 2H, CH_2), 4.39 (t, 2H, $J = 3.6$ Hz, CH_2), 7.93 (s, 1H, imi-H), and 8.47 (s, 1H, imi-H). ESI-HRMS calcd for $C_6H_7N_4O_2$ $[M + H]^+$ 167.0564, found 167.0532. Anal. Calcd for $C_6H_6N_4O_2$: C, 43.38; H, 3.64; N, 33.72; found C 43.83, H 3.57, N 33.40. 1-(2-Cyanoethyl)-4-nitroimidazole (0.83 g, 5 mmol), and hydroxylamine (0.66 g, 20 mmol), were mixed in 10 mL methanol, and the mixture was stirred at room temperature for 10 h. The mixture was placed at 0 °C overnight, and a white crystalline powder precipitated. It was further purified by recrystallization from water, to a pale green crystals, yield 75%. m.p. 145.0–146.0 °C; ^1H NMR (CD_3OD, 500 MHz) δ: 2.4–2.6 (m, 4H, NH_2 and CH_2), 4.2 (t, 2H, $J = 3.6$ Hz, CH_2), 7.63 (s, 1H, imi-H), 8.11 (s, 1H, imi-H). 8.38 (s, 1H, N–OH). ^{13}C NMR (CD_3OD, 500 MHz) δ:31.98, 44.51, 121.67, 137.50, 146.77, and 149.40. ESI-HRMS calcd for $C_6H_{10}N_5O_3$ $[M + H]^+$ 200.0778, found 200.0772. Anal. Calcd for $C_6H_9N_5O_3$: C, 36.18; H, 4.55; N, 35.16; found C, 36.25; H, 4.52; N, 35.41.

^{99m}Tc-N4IPA was synthesized as follows: N4IPA solution (200 μL, 1 mg/mL) and sodium tartrate solution (25 μL, 1 mg/mL) were added into 1 mL of 0.1 M PBS (pH = 7.4). Then freshly prepared stannous chloride solution (10 μL, 1 mg/mL) and 370 MBq $^{99m}TcO_4^-$ was added. The mixture was shaken vigorously and heated to 75 °C for 15 min. Radio-TLC or Radio-HPLC showed radiolabeling yield and radiochemical purity >95% and >98%.

2.2. Evaluation of ^{99m}Tc-N4IPA

2.2.1. Partition coefficient of ^{99m}Tc-N4IPA

The partition coefficient of ^{99m}Tc-N4IPA complex was determined by measuring the distribution of radioactivity in 1-octanol and 0.01 M PBS. Concisely, a 10 μL sample of ^{99m}Tc-N4IPA in PBS was added to a vial which contained 1 mL of 1-octanol and 0.99 mL of PBS. After the mixture had been vortexes for 8 min, the vial was centrifuged for 5 min to ensure complete separation of layers. Then, 10 μL of each layer was pipetted into the test tubes, to calculate log P = log (counts in octanol/counts in water) [19].

2.2.2. The in vitro stability of ^{99m}Tc-N4IPA

The radiochemical purity measured by radio-HPLC at different times after preparation represent the in vitro stability of the radioligand. ^{99m}Tc-N4IPA (0.2 mL, 14.8 MBq) was added to a test tube with 1 mL 0.1 M PBS. The mixture was incubated by shaking the test tube at 25 and 37 °C in a water bath. The radiochemical purity was measured at 10 min, 1, 2, 4, 8 and 12 h by radio-HPLC. The same experiment was repeated while 5% BSA was added in the incubation mixture.

2.2.3. Blood retention of ^{99m}Tc-N4IPA in mice

^{99m}Tc-N4IPA (0.2 mL, 14.8 MBq) was injected intravenously into the tail vein of healthy female BABL/c mice (18–22 g, $n = 7$), 10 μL blood was collected at a different location of the tail vein at 2 min, 15 min, 30 min, 1, 2, 4, 6, 8, 11, 21, 24 h post injection. The radioactivity of the samples was measured with a γ counter. The blood retention of ^{99m}Tc-N4IPA was expressed as percentage of injected dose per gram of tissue (%ID/g).

2.3. In vitro cell uptake of ^{99m}Tc-N4IPA

The internalization of ^{99m}Tc-N4IPA in CHO tumor cells was performed as described [20,21]. CHO cells were grown in suspension at 37 °C in DMEM plus 10% fetal calf serum, were spun down from suspension and resuspended in fresh medium at the desired cell density (1×10^6/mL). Cells (20 mL) were equilibrated for 45 min in special glass vials with stirring at 37 °C under a continuous flow of a pre-humidified gas mixture of 95% N_2 + 5% CO_2 (hypoxia exposure) or 95% air + 5% CO_2 (aerobic exposure). After equilibration, ^{99m}Tc-N4IPA (0.2 mL, 14.8 MBq) was added to make the final radioactivity of 0.25 MBq/mL in each vial. After 5 min, 1, 2, 3, 4 h, samples (0.2 mL, 5 repeat each) were removed from the vials to 1 mL centrifugal tubes without disturbing the oxygenation status of cells in the vials. Those vials were centrifugated at 1500 r/min for 5 min, to separate the cells from the supernatant. 180 μL of the supernatant was carefully aspirated, and its radioactivity was counted as that in the supernatant (Cs), and the remaining 20 μL of the samples was counted as that the residual (Cr). The percentage of radioactivity uptake in cells was calculated as follows: uptake = (Cr − Cs/9)/(Cr + Cs) × 100%. Cell viability was confirmed by methylene blue staining before and after the uptake experiment, to be greater than 90% as the requirement of the experiment.

2.4. Biodistribution of ^{99m}Tc-N4IPA

A suspension of U87 cells (human glioma) or A549 cells (human lung cancer) in 0.1 mL (1×10^7/mL) was injected subcutaneously at the left axilla of six week-old BALB/c mice (female, 20–25 g). When

the diameter of the tumor reached 0.5–1.5 cm (weight 75–1200 mg), the biodistribution experiments would be performed.

2.4.1. Biodistribution of ^{99m}Tc-N4IPA in U87-bearing BALB/c mice

Nine glioma U87-bearing BALB/c mice were divided into three groups. Each mouse received an intravenous injection of ^{99m}Tc-N4IPA (0.1 mL, 1.85 MBq) via tail vein, and was sacrificed by cervical dislocation at 15 min, 2, 4 h post injection. Tissue or organ samples including blood, heart, liver, spleen, lung, kidney, stomach, intestine, muscle, bone and tumor were removed, weighed, and counted with a γ counter. The radioactivity uptake was calculated as the percentage of injected dose per gram of tissue (%ID/g).

2.4.2. Biodistribution of ^{99m}Tc-N4IPA in A549-bearing BALB/c mice

This study was performed analogously as that in U87-bearing mice, but three series of A549 bearing BALB/c mice were selected according to the tumor weight, with the diameter of the tumor about 0.6 ± 0.2 cm (tumor weight about 75–200 mg, about 5 weeks) as small tumor, about 1.0 ± 0.2 cm (tumor weight about 200–600 mg, about 6 weeks) as medium tumor, and about 1.4 ± 0.2 cm (tumor weight about 600–1200 mg, about 7 weeks) as large tumor.

2.5. SPECT imaging of ^{99m}Tc-N4IPA

2.5.1. SPECT imaging of ^{99m}Tc-N4IPA in U87-bearing BALB/c mice

Glioma U87-bearing BALB/c mice were placed in supine and fixed, and each was injected with ^{99m}Tc-N4IPA (0.1 ml, 18.5 MBq) via tail vein. Static images were acquired by a SPECT at 10 min, 1, 2, 4, 24 h post injection. The following parameters were used: low-energy high-resolution collimator, energy peak: 140 keV; window width: 15%; matrix: 128 × 128; zoom = 3.2; counts: 500 k per view. The tumor to non-tumor ratio was calculated using region of interest (ROI) at the tumor site versus that at the opposite axilla without tumor.

2.5.2. SPECT imaging of ^{99m}Tc-N4IPA in A549-bearing BALB/c mice

Three sets of A549-bearing BALB/c mice selected according to different tumor weight (A: Small; B: Medium; C: Large) were used for this study. Static images were acquired at 4 h post injection. Other steps of the procedure were the same as those used for U87-bearing mice.

2.6. Autoradiography and immunohistochemistry analysis of ^{99m}Tc-N4IPA in tissue hypoxia

In order to create immunohistochemical response from tissue hypoxia, hypoxyprobe-1 (pimonidazole, 1.0 mg) was dissolved in 0.2 mL brine, and was injected via tail vein into three glioma U87-bearing BALB/c mice with the diameter of their tumors at

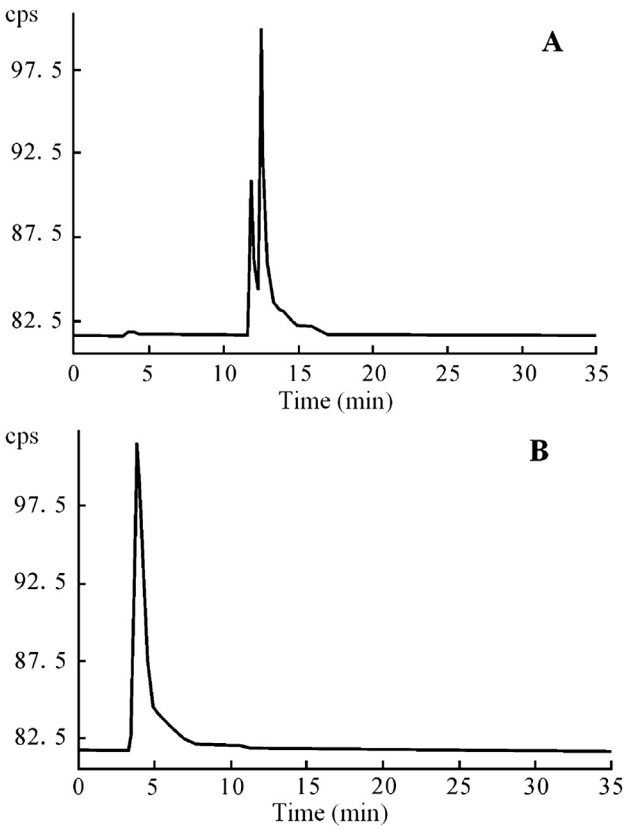

Fig. 1. HPLC analysis. A: ^{99m}Tc-N4IPA; B: Na^{99m}TcO$_4$.

1.0 ± 0.2 cm. Twenty hours later, these mice were injected intravenously with ^{99m}Tc-N4IPA (0.1 mL, 18.5 MBq), and were sacrificed by cervical dislocation at 2 h post injection. After killing, tumors were quickly dissected, frozen to −40 °C, and sectioned consecutively at 10 μm thickness slices.

2.6.1. Autoradiography and hematoxylin eosin staining

The tumor tissue slices were air dried at 40 °C, and then exposed on high-sensitivity imaging film overnight. Autoradiographic images were analyzed with a computerized imaging analysis system. After autoradiography, the frozen tissue slices were washed by distilled water, and then were stained with hematoxylin and eosin to show different structure of the tissue.

2.6.2. Immunohistochemistry of tissue hypoxia

Standard protocol for the detection of tissue hypoxia was followed. In order to block internal peroxidase from staining, the

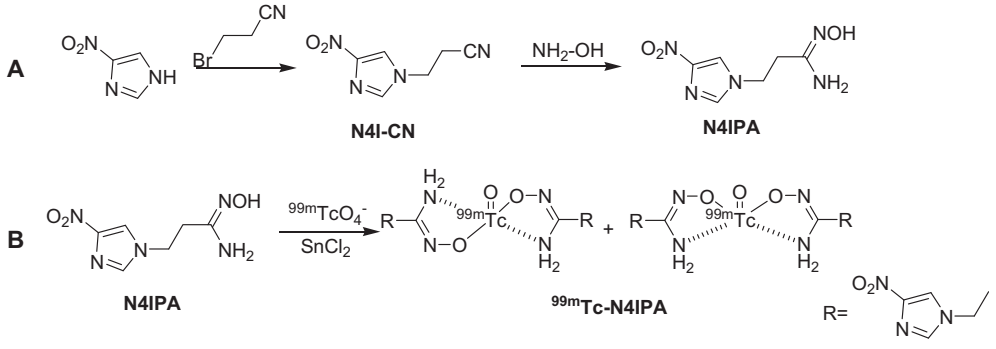

Scheme 1. Synthetic strategy for A) N4IPA and B) radiolabeling of ^{99m}Tc-N4IPA isomers.

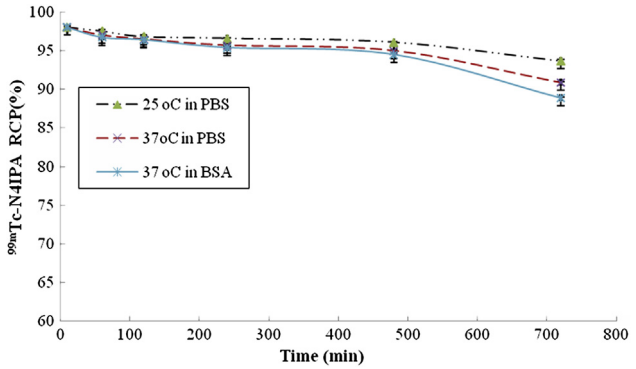

Fig. 2. In vitro stability of ^{99m}Tc-N4IPA.

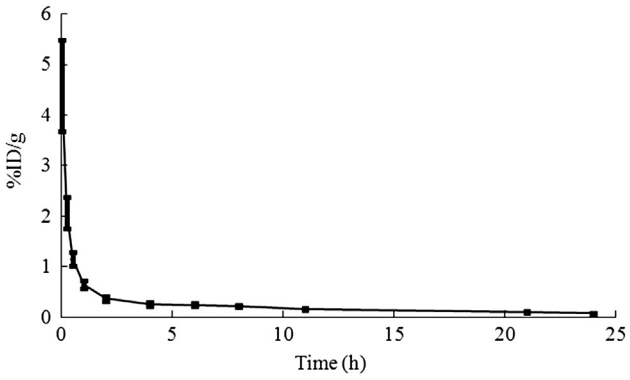

Fig. 4. Blood retention curve of ^{99m}Tc-N4IPA.

frozen tissue slices were dipped in 3% H_2O_2 solution at room temperature for 5 min. They were putted into 0.01% pronase at 40 °C for 40 min for antigen retrieval, and cooled naturally. After the slides were washed by 0.01 M PBS at 2 min each for three times, they were washed by Dako blocking solution to block non-specific binding for 5 min. The slices were incubated in Hypoxyprobe-1MAb1 (1:50) for 40 min at room temperature, and washed by 0.01 M PBS for three times. They were incubated in a second antibody-Biotin-conjugated F(ab')2 (1:500) for 10 min at room temperature, and were washed by 0.01 M PBS for three times. The bound antibody was visualized by the DAB-kit for 10 min. The slides incubated with 0.01 M PBS instead of Hypoxyprobe-1MAb1 were used as negative control, while samples provided by the Hypoxyprobe-1 kit company were used as positive control. Yellow or brown granules in cytoplasm or karyon were considered as positive staining.

2.7. Statistical analysis

Cell uptake and biodistribution data were analyzed using two-tailed, unpaired student *t*-tests, with *p* values less than 0.05 considered to be statistically significant. The in vitro percentage of radiotracer uptake, in vivo percentage of injected radiotracer dose per gram of tissue, and tumor to non-tumor ratios are presented as the mean ± standard deviation. These statistical computations were performed using the Excel software program (Microsoft Corporation, Redmond, WA).

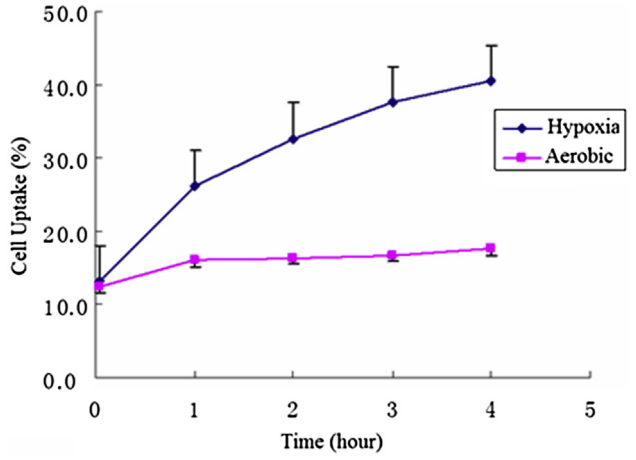

Fig. 3. Accumulation of ^{99m}Tc-N4IPA in CHO cells under hypoxic/aerobic conditions ($X \pm s$, $n = 5$).

3. Results

3.1. Synthesis of radiolabeled ^{99m}Tc-N4IPA

The synthesis of radiolabeled ^{99m}Tc-N4IPA were completed in 3 steps (Scheme 1). 3-Bromopropionitrile, instead of Acrylonitrile, reacted with 4-nitroimidazole in the presence of triethylamine, to generate 1-(2-cyanoethyl)-4-nitroimidazole, which was purified by recrystallization with high yield of 80%. The nitrile product reacted with hydroxylamine to prepare N4IPA [10]. ^{99m}Tc-N4IPA was prepared by reacting N4IPA with $^{99m}TcO_4^-$ under reducing conditions, according to the reconstituting lyophilization kit. The radioactive peaks on radio-HPLC corresponding to products and starting material are well separated (Fig. 1), the retention time of the products as a doublet at 12 and 12.9 min, and starting material $^{99m}TcO_4^-$ at 4.0 min. The isolated radiolabeled compounds were >95% purity.

3.2. In vitro properties of ^{99m}Tc-N4IPA

3.2.1. Partition coefficient of ^{99m}Tc-N4IPA

In order to evaluate the lipophilicity of ^{99m}Tc-N4IPA, we measured its partition coefficient in octanol/water to be ($P_{O/W}$) 2.71 ± 0.05. This is lower than that of ^{99m}Tc-BMS181321 at $P_{O/W} = 40.3$ [22], but is still in the right range for tissue permeability.

3.2.2. In vitro stability of ^{99m}Tc-N4IPA

In vitro stability of ^{99m}Tc-N4IPA was evaluated in PBS and BSA solution. Both solutions were incubated at 37 °C within 6 h. No decomposition or dissociation of the complexes was observed (Fig. 2).

Table 1
Biodistribution of ^{99m}Tc-N4IPA in each A549 beard Balb/c mice (Tumor weight about 75–200 mg).

Tissue	%ID/g		
	15 min ($n = 3$)	2 h ($n = 3$)	4 h ($n = 3$)
Blood	0.73 ± 0.21	0.30 ± 0.06	0.21 ± 0.00
Heart	0.42 ± 0.36	0.28 ± 0.08	0.20 ± 0.08
Liver	1.44 ± 0.70	0.82 ± 0.11	0.57 ± 0.16
Spleen	0.61 ± 0.35	0.30 ± 0.13	0.30 ± 0.08
Kidney	2.86 ± 1.35	1.53 ± 0.23	1.01 ± 0.15
Lung	0.72 ± 0.16	0.28 ± 0.01	0.12 ± 0.05
Stomach	0.56 ± 0.18	0.32 ± 0.16	0.21 ± 0.02
Intestine	0.64 ± 0.30	0.40 ± 0.17	0.23 ± 0.02
Muscle	0.19 ± 0.06	0.06 ± 0.01	0.04 ± 0.00
Bone	0.51 ± 0.16	0.27 ± 0.03	0.17 ± 0.01
Tumor	0.66 ± 0.21	0.40 ± 0.12	0.37 ± 0.09
Tumor (mg)	**128.03 ± 71.96**	**118 ± 23.05**	**126.57 ± 56.61**

Table 2
Biodistribution of ^{99m}Tc-N4IPA in each A549 beard Balb/c mice (Tumor weight about 200–600 mg).

Tissue	%ID/g		
	15 min ($n = 3$)	2 h ($n = 3$)	4 h ($n = 3$)
Blood	0.73 ± 0.11	0.28 ± 0.04	0.20 ± 0.06
Heart	0.53 ± 0.05	0.24 ± 0.02	0.17 ± 0.03
Liver	1.55 ± 0.74	0.84 ± 0.05	0.34 ± 0.03
Spleen	0.25 ± 0.12	0.15 ± 0.01	0.08 ± 0.09
Kidney	2.90 ± 0.36	1.23 ± 0.11	0.93 ± 0.09
Lung	0.34 ± 0.19	0.12 ± 0.04	0.06 ± 0.07
Stomach	0.35 ± 0.09	0.21 ± 0.03	0.20 ± 0.07
Intestine	0.39 ± 0.13	0.23 ± 0.03	0.23 ± 0.03
Muscle	0.19 ± 0.02	0.04 ± 0.01	0.03 ± 0.01
Bone	0.34 ± 0.02	0.15 ± 0.02	0.07 ± 0.03
Tumor	0.43 ± 0.02	0.31 ± 0.10	0.22 ± 0.05
Tumor (mg)	**581.73 ± 63.58**	**414.43 ± 87.34**	**341.43 ± 78.00**

Table 4
Comparison of biodistribution of ^{99m}Tc-N4IPA in A549 beard Balb/c mice in different tumor weight.

Time	Type	Tumor diameter			*P* value
		0.6 ± 0.2 cm	1.0 ± 0.2 cm	1.4 ± 0.2 cm	
15 min	T/B	0.90 ± 0.21	0.60 ± 0.11	0.57 ± 0.09	0.111
	T/M	3.44 ± 0.81	2.24 ± 0.19	2.42 ± 0.69	0.192
	Tumor (mg)	128.03 ± 71.96	581.73 ± 63.58	771 ± 55.15	0.014
2 h	T/B	1.33 ± 0.36	1.09 ± 0.35	1.14 ± 0.30	0.733
	T/M	7.66 ± 3.66	8.05 ± 1.40	8.34 ± 3.45	0.974
	Tumor (mg)	118 ± 23.05	414.43 ± 87.34	817.07 ± 78.42	0.003
4 h	T/B	1.72 ± 0.40	1.25 ± 0.58	1.04 ± 0.27	0.279
	T/M	8.96 ± 1.85	8.48 ± 4.51	8.95 ± 1.68	0.978
	Tumor (mg)	126.57 ± 56.61	341.43 ± 78.00	687.2 ± 50.27	0.019

3.3. Accumulation of ^{99m}Tc-N4IPA in CHO cells

The accumulation of ^{99m}Tc-N4IPA in CHO cell suspension was evaluated under both aerobic and hypoxic conditions at 37 °C (Fig. 3). After short incubation time of 5 min, the cell uptakes were not statistically different ($P = 0.304$), with uptake of (12.48 ± 5.16)% for aerobic conditions and (13.15 ± 3.78)% for hypoxic conditions, respectively. However, after 4 h of incubation, the uptake in aerobic conditions was almost no change, while that in hypoxic conditions increased with time, and reached (40.56 ± 6.44)%.

3.4. Biodistribution studies

3.4.1. Blood retention of ^{99m}Tc-N4IPA in mice

Blood retention of ^{99m}Tc-N4IPA in mice follows a typical blood retention pattern of small- molecule compounds, with rapid rise of radioactivity and fast washout (Fig. 4). The curve can be fitted with a two-compartment model, $y = 4.55 \times e^{-2.82t} + 0.33 \times e^{-0.068t}$ ($R^2 = 0.9921$), with the half life of distribution phase ($T_{1/2\alpha}$) at 0.25 h and that of elimination ($T_{1/2\beta}$) at 10.2 h, respectively. The in vivo stability of ^{99m}Tc-N4IPA in mouse blood was followed by radio-HPLC. No decomposition was observed within 60 min post injection.

3.4.2. Biodistribution of ^{99m}Tc-N4IPA in Balb/c mice bearing A549 tumor cells

The biodistribution of ^{99m}Tc-N4IPA in Balb/c mice bearing A549 tumor cells for 3 different tumor sizes (small, medium, large) followed the same pattern (Tables 1–3). At 15 min post injection, uptake of ^{99m}Tc-N4IPA in blood was only about 0.7%, with a rapid blood clearance during the next 4 h to 0.2% ID/g. Kidney had the highest uptake among all tissues, followed by liver and intestine, suggesting that ^{99m}Tc-N4IPA was mainly excreted from the urinary system and partly excreted from the hepato-intestinal system, consistent with the lipophilic character of the radioligand. Except these 3 organs, the uptake of other organs was very low. Compared with most organs, ^{99m}Tc-N4IPA uptake in tumor was relatively high, and the decline of the radioactivity in tumor was slow (Tables 1–3).

Statistical analysis of the uptake ratios, tumor/blood (T/B) and tumor/muscle (T/M), showed no difference ($p > 0.05$) among 3 groups of Balb/c mice bearing A549 tumor cells with different tumor size at 15 min, 2 h and 4 h post injection (Table 4). The hypoxic part of a tumor can be characterized by the maximum tumor/blood (T/B) and tumor/muscle (T/M), while tumor hypoxia appears to be strongly associated with tumor propagation and malignant progression.

3.4.3. Biodistribution of ^{99m}Tc-N4IPA in Balb/c mice bearing U87

The biodistribution of ^{99m}Tc-N4IPA in Balb/c mice bearing U87 tumor cells for 3 different tumor sizes (small, medium, large) followed the same pattern (Table 5). At 15 min post injection, the uptake of ^{99m}Tc-N4IPA in blood was only 0.69%, with a rapid blood clearance comparing with 4 h to 0.2%. Kidney had the highest uptake among all tissues, followed by the liver and the intestine, suggesting that ^{99m}Tc-N4IPA was mainly excreted from the urinary system, consistent with the characteristics of lipophilic compounds. The decline of the radioactivity in tumor was slow, compared with those from other tissues. Both ratios of tumor-to-

Table 3
Biodistribution of ^{99m}Tc-N4IPA in each A549 beard Balb/c mice (Tumor weight about 600–1200 mg).

Tissue	%ID/g		
	15 min ($n = 3$)	2 h ($n = 3$)	4 h ($n = 3$)
Blood	0.71 ± 0.03	0.24 ± 0.02	0.19 ± 0.01
Heart	0.58 ± 0.29	0.21 ± 0.05	0.17 ± 0.01
Liver	1.34 ± 0.06	0.78 ± 0.22	0.28 ± 0.03
Spleen	0.25 ± 0.02	0.13 ± 0.03	0.10 ± 0.01
Kidney	3.46 ± 1.01	1.20 ± 0.19	0.97 ± 0.09
Lung	0.28 ± 0.10	0.17 ± 0.01	0.05 ± 0.00
Stomach	0.32 ± 0.12	0.21 ± 0.05	0.20 ± 0.03
Intestine	0.45 ± 0.18	0.22 ± 0.05	0.22 ± 0.04
Muscle	0.17 ± 0.03	0.04 ± 0.01	0.02 ± 0.01
Bone	0.22 ± 0.02	0.13 ± 0.02	0.12 ± 0.02
Tumor	0.40 ± 0.07	0.28 ± 0.08	0.20 ± 0.04
Tumor (mg)	**771 ± 55.15**	**817.07 ± 78.42**	**687.2 ± 50.27**

Table 5
Biodistribution of ^{99m}Tc-N4IPA in mice bearing human glioma U87 (mean ± SD, $n = 3$).

Tissue	%ID/g		
	15 min	2 h	4 h
Blood	0.69 ± 0.07	0.30 ± 0.02	0.20 ± 0.02
Heart	0.34 ± 0.04	0.23 ± 0.01	0.17 ± 0.01
Liver	1.81 ± 0.13	1.04 ± 0.12	0.83 ± 0.15
Spleen	0.36 ± 0.12	0.30 ± 0.02	0.26 ± 0.03
Kidney	5.41 ± 1.73	4.15 ± 0.72	3.46 ± 0.73
Lung	0.55 ± 0.03	0.28 ± 0.01	0.25 ± 0.02
Stomach	0.54 ± 0.12	0.42 ± 0.03	0.31 ± 0.08
Intestine	0.61 ± 0.12	0.48 ± 0.11	0.35 ± 0.08
Muscle	0.19 ± 0.09	0.04 ± 0.00	0.03 ± 0.00
Bone	0.13 ± 0.01	0.13 ± 0.01	0.12 ± 0.02
Tumor	0.61 ± 0.16	0.46 ± 0.07	0.40 ± 0.01
Tumor (mg)	**444.93 ± 43.35**	**434.53 ± 43.74**	**356.07 ± 30.24**

Table 6
The comparison of the biodistribution of ^{99m}Tc-N4IPA in Balb/c mice bearing A549 and U87 tumor cells in different time points.

Time	Type	Tumor cell		*P* value
		U87	A549	
15 min	T/B	0.88 ± 0.21	0.60 ± 0.11	0.166
	T/M	4.02 ± 1.94	2.24 ± 0.19	0.324
	Tumor (mg)	444.93 ± 43.35	581.73 ± 63.58	0.67
2 h	T/B	1.57 ± 0.31	1.09 ± 0.35	0.181
	T/M	11.89 ± 1.64	8.05 ± 1.40	0.053
	Tumor (mg)	434.53 ± 43.74	414.43 ± 87.34	0.92
4 h	T/B	1.98 ± 0.25	1.25 ± 0.58	0.123
	T/M	13.11 ± 1.47	8.48 ± 4.51	0.174
	Tumor (mg)	356.07 ± 30.24	341.43 ± 78.00	0.92

blood ratio (T/B) and tumor-to-muscle ratio (T/M) increased within 4 h, reaching 0.88, 1.57 and 1.98, respectively, for T/B, and reaching 4.02, 11.89 and 13.11, respectively, for T/M, at 15 min, 2 h, and 4 h, post injection.

No statistical difference ($p > 0.05$) between the T/B ratio and T/M ratio existed in the two animal models in this study (Table 6). This means that ^{99m}Tc-N4IPA uptake is independent of tumor size and tumor weight.

3.5. SPECT imaging of ^{99m}Tc-N4IPA

3.5.1. SPECT imaging of ^{99m}Tc-N4IPA in Balb/c mice bearing U87 tumor cells

The radioactivity of the tumor was higher than that of the reference side as early as 10 min after the injection of the radioligand, and the image of the tumor became clearer with time until 4 h after injection (Fig. 5). The region of interest (ROI) was used for semi-quantitative analysis of the radioactivity in tumor, and tumor/background (T/B) ratios at 5 min, 1, 2, 4 and 22 h, were 1.23 ± 0.07, 1.89 ± 0.08, 2.17 ± 0.08, 3.44 ± 0.13 and 1.51 ± 0.1 ($n = 3$), respectively. The radioactivity of the abdomen was higher than that of the head, and no radioactivity in the region of thyroid and the stomach was observed, suggesting no dissociative $^{99m}TcO_4^-$.

3.5.2. SPECT imaging of ^{99m}Tc-N4IPA in Balb/c mice bearing A549 tumor cells

The SPECT imaging of three groups of Balb/c mice bearing A549 tumor cells with different tumor weight (Fig. 6) showed clear uptake increase in tumors at 4 h after intravenous injection of ^{99m}Tc-N4IPA (Fig. 4). Relatively high radioactivity of ^{99m}Tc-N4IPA in kidney and bladder was observed, but no radioactivity was observed in the region of thyroid.

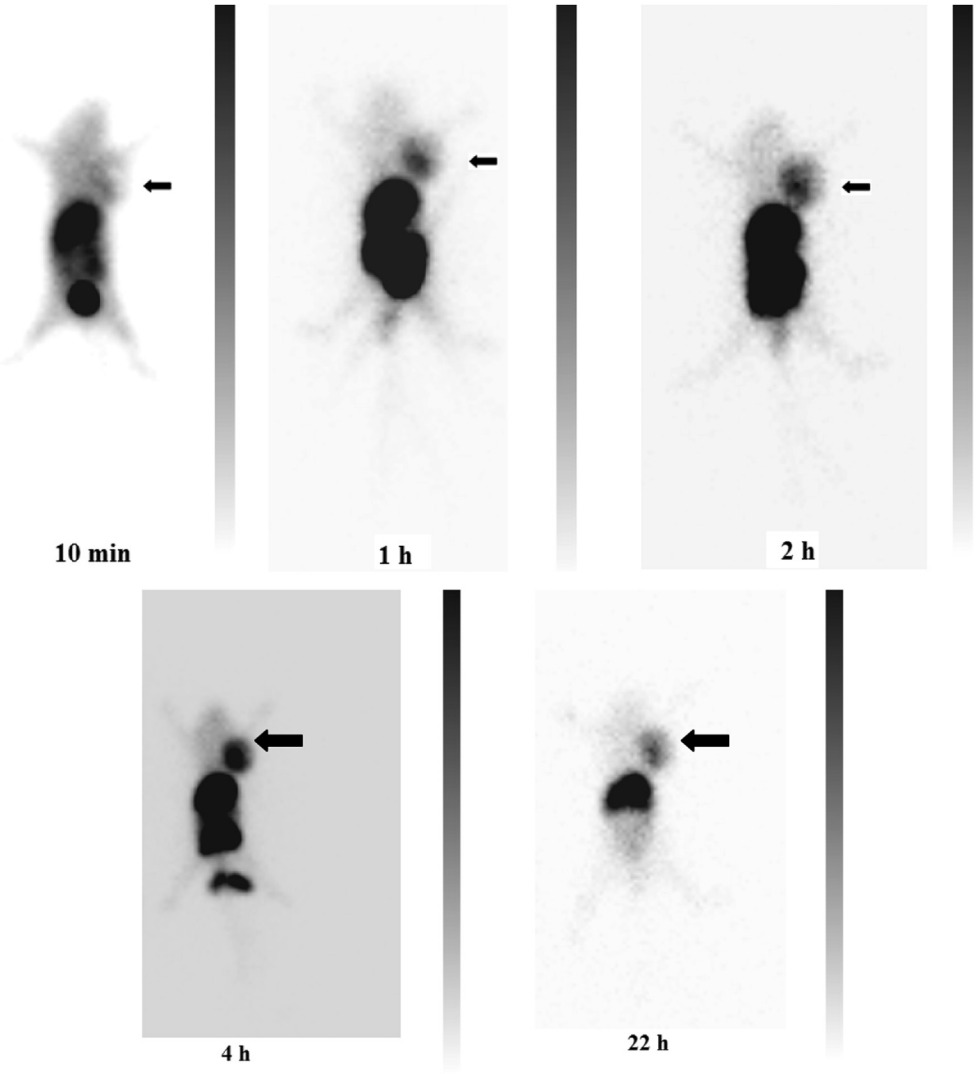

Fig. 5. Static SPECT images of a Balb/c mouse bearing U87 tumor cells at five different time intervals after injection of ^{99m}Tc-N4IPA (arrow indicates tumor).

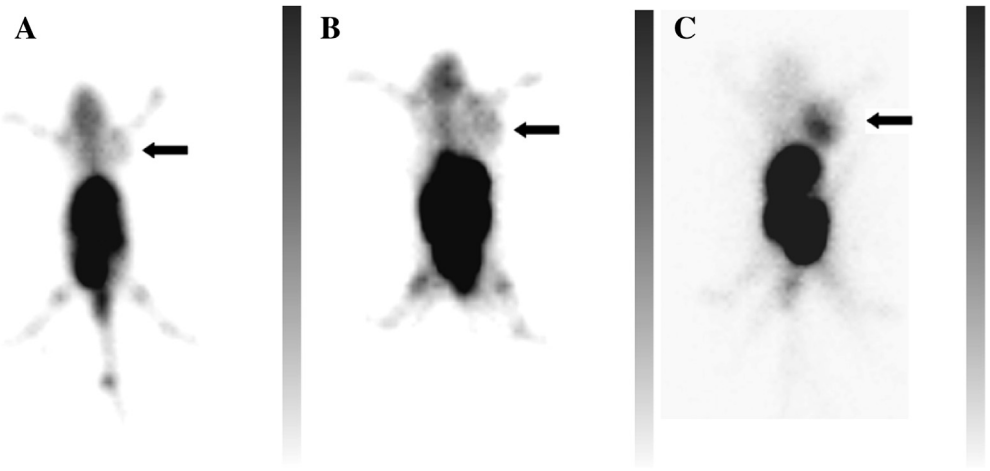

Fig. 6. Static SPECT images of a Balb/c mouse bearing A549 tumor cells with different tumor weight (A. Small; B. Medium; C. Large) at 4 h after injection of ^{99m}Tc-N4IPA (arrow indicates tumor).

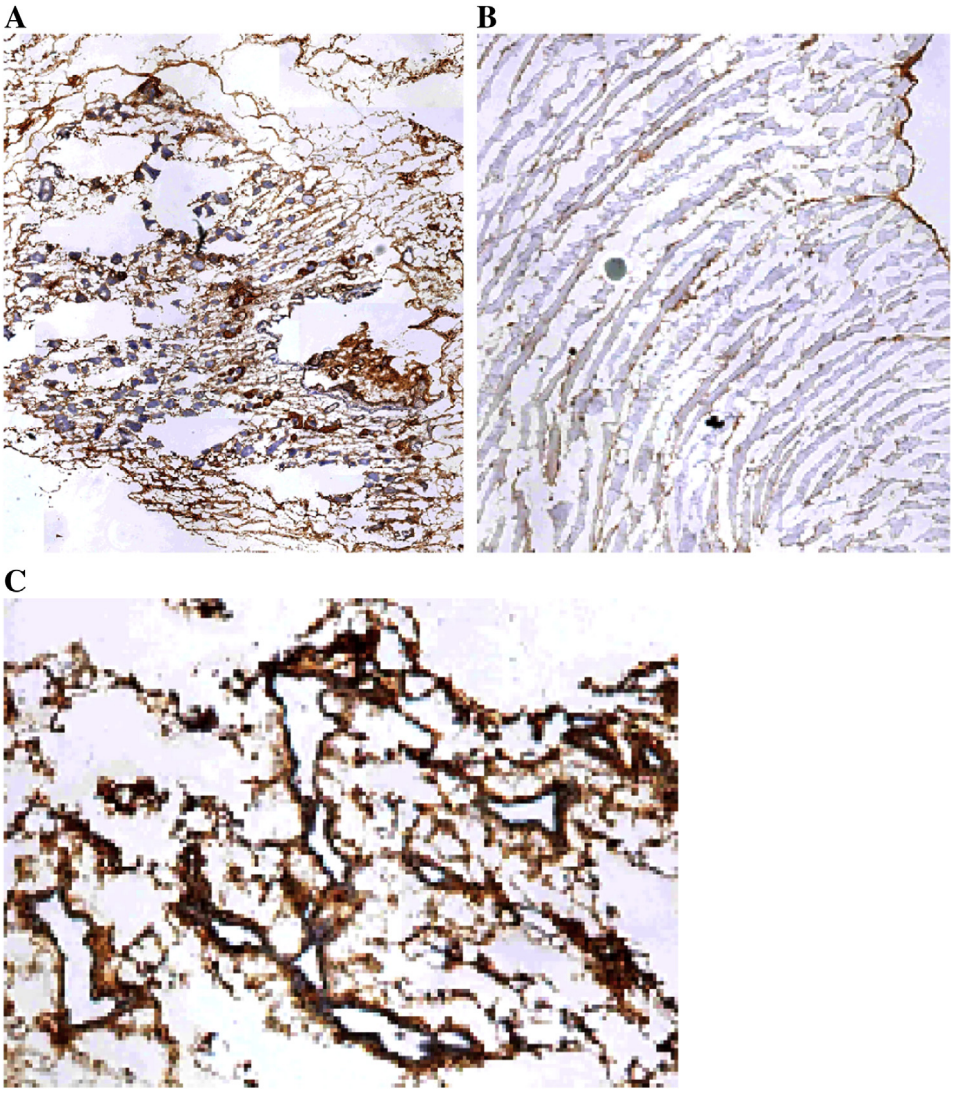

Fig. 7. Pictures stained with hypoxyprobe-1 in different regions of the same tumor tissue: A) in regions of diffuse tumor cells; B) in the bleeding regions; C) in the regions of liquescence and necrosis.

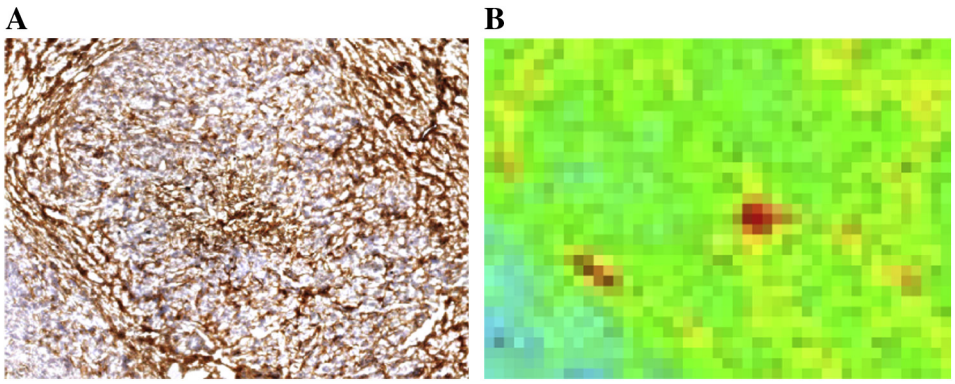

Fig. 8. Comparison of A) immunohistochemical stain with hypoxyprobe-1, and B) autoradiogram of ^{99m}Tc-N4IPA when tumor cells got together as nodus. 200× magnifications of original micrographs.

3.6. Autoradiography and immunohistochemistry

The pattern stained with hypoxyprobe-1 depends on the regions of the tumor tissue bearing U87 tumor cells (Fig. 7): no stain in regions of bleeding (first region), light stain in regions of diffuse tumor cells (second region), and heavy stain in regions of liquescence and the necrosis (third region), which are believed to be the hypoxic area. When tumor cells got together as a node, the center region was also heavily stained with ^{99m}Tc-N4IPA (Fig. 8). The pattern of the autoradiogram of ^{99m}Tc-N4IPA followed that stained with hypoxyprobe-1 in the first and second regions, but not in the third region (Fig. 9).

4. Discussion

Synthesis and characterization of ^{99m}Tc-N4IPA. The synthesis of N4IPA precursor was completed in 2 steps. The radiolabeling was achieved in one step with high radiochemical yield. HPLC analysis of ^{99m}Tc-N4IPA showed 2 peaks, consistent with isomers of ^{99m}Tc-complexes (Scheme 1). Nakayama et al., also observed 2 peaks in the HPLC analysis of the ^{99m}Tc-hydroxyiminoamide complexes containing phenyl group [18].

Specificity of ^{99m}Tc-N4IPA for hypoxia. In order to verify the hypoxic selectivity of ^{99m}Tc-N4IPA, we have studied its specificity both in CHO cells and in mice. The cell uptake under hypoxic conditions was all higher than that under aerobic conditions at 1, 2, 3, 4 h incubation time ($p < 0.05$), consistent with previous studies of ^{99m}Tc-BMS181321 and ^{99m}Tc-BRU59-21 in the same cell line. Hypoxyprobe-1, a 2-nitroimidazole hypoxia marker, has been widely used in practice as a reliable method to measure hypoxia at both cellular level and tissue level. After intravenous injection, hypoxyprobe-1 can distribute to all tissues in the body, including brain, but it binds only to cells with less than 14 μM of dioxygen concentrations, equivalent to a pO2 of 10 mmHg at

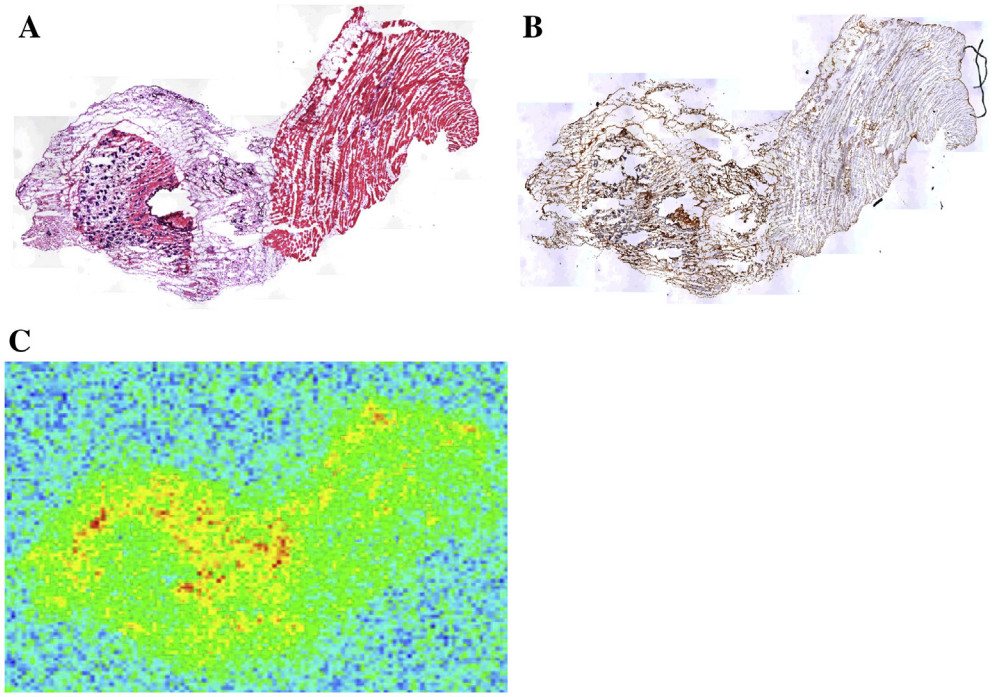

Fig. 9. A) Hematoxylin and eosin stain (HE stain); B) hypoxyprobe-1 immunohistochemical stain; C) autoradiogram in tumor 4 h post radiotracer injection. 2× magnifications of original micrographs.

Table 7
Comparison of some technetium labeled hypoxic agents.

Compounds	$P_{O/W}$	ID%/g (2 h)			T/B	T/M	Tumor model
		Tumor	Blood	Muscle			
^{99m}Tc-BRU59-21 [7]	11.0	0.37	0.43	0.09	0.86	3.84	C3H/HeJ mice bearing syngenic fibrosarcoma KTH
^{99m}Tc-HL91 [8]	0.08	0.89	–	–	2.22	4.34	Wistar rats bearing syngenic rat mammary cancer
^{99m}Tc-BMS181321 [22]	40.3	0.55	1.75	0.19	0.31	2.63	C3H/HeJ mice bearing syngenic fibrosarcoma KTH
^{99}Tc^{m}-N4IPA	2.7	0.46	0.30	0.04	1.57	11.89	Balb/c mice bearing human glioma U87

37 °C. The results of hypoxic measurement by hypoxyprobe-1 were also confirmed by other methods [23,24]. The autoradiogram of ^{99m}Tc-N4IPA follows the pattern obtained from immunohistochemistry with hypoxyprobe-1. This confirms that ^{99m}Tc-N4IPA selectively reflects the hypoxic activity in tissue level in vivo.

SPECT imaging of ^{99m}Tc-N4IPA. ^{99m}Tc-N4IPA showed rapid blood clearance, fairly low muscles uptake, and relatively high tumor accumulation (Figs. 5 and 6). No statistical difference ($p > 0.05$) between the T/B and T/M ratio have been observed between the two animal models and among different sizes of tumor in one animal model. ^{99m}Tc-N4IPA has less excretion from hepato-intestine system and less uptake of brain than those of ^{99m}Tc-labeled nitroimidazole-containing image agents in clinical use (such as ^{99m}Tc-BMS181321 and ^{99m}Tc-BRU59-21), probably from their differences in lipophilicity, with $P_{O/W}$ 2.71 ± 0.05 vs $P_{O/W}$ 40.3 ± 2.2 and 11.0 ± 0.8, respectively (Table 5). These results suggested that tumor tissues may be more effectively visualized by ^{99m}Tc-N4IPA than those by the other two agents (Table 7).

5. Conclusion

We have synthesized and evaluated ^{99m}Tc-N4IPA as an imaging agent for hypoxia in tumor both in vitro and in vivo. The radiolabeling was straightforward and in high yield, and ^{99m}Tc-N4IPA showed in vitro/vivo stability. ^{99m}Tc-N4IPA accumulated more in cells in hypoxic conditions than in aerobic conditions. The specificity of ^{99m}Tc-N4IPA for hypoxia in vivo was confirmed by the close match between ex vivo autoradiography and immunohistochemical stain by hypoxyprobe-1. SPECT imaging of ^{99m}Tc-N4IPA in nude mice bearing U87 and A549 tumor cells showed clear imaging of tumors, with high T/B and T/M ratios, irrespective of tumor sizes. ^{99m}Tc-N4IPA has much more favorable pharmacokinetics than those of ^{99m}Tc-BMS181321 and ^{99m}Tc-BRU59-21, most probably from less lipophilicity as reflected in octanol/water partition coefficient. These results make ^{99m}Tc-N4IPA a potential imaging agent for hypoxia in clinical use, worth further study.

Acknowledgments

We thank the National Natural Science Foundation of China (No. 81371592, No. 81071198 and No. 81172082) and the Beijing Natural Science Foundation (No. 7052015 and No. 7132040) for financial support.

References

[1] T.G. Graeber, C. Osmanian, T. Jacks, D.E. Housman, C.J. Koch, S.W. Lowe, A.J. Giaccia, Nature 379 (1996) 88–91.
[2] P. Vaupel, A. Mayer, Cancer Metastasis Rev. 26 (2007) 225–239.
[3] A. Nunn, K. Linder, H.W. Strauss, Eur. J. Nucl. Med. 22 (1995) 265–280.
[4] G.J. Cook, I. Fogelman, Eur. J. Nucl. Med. 25 (1998) 335–337.
[5] D.S. Cowan, T. Melo, L. Park, J.R. Ballinger, A.M. Rauth, Br. J. Cancer 27 (1996) S264–S266.
[6] C.Q. Shi, A.J. Sinusas, D.P. Dione, M.J. Singer, L.H. Young, E.N. Heller, B.D. Rinker, F.J. Wackers, B.L. Zaret, J. Nucl. Med. 36 (1995) 1078–1086.
[7] T. Melo, J. Duncan, J.R. Ballinger, A.M. Rauth, J. Nucl. Med. 41 (2000) 169–176.
[8] K. Yutani, H. Kusuoka, K. Fukuchi, M. Tatsumi, T. Nishimura, J. Nucl. Med. 40 (1999) 854–861.
[9] T. Chu, R. Li, S. Hu, X. Liu, X. Wang, Nucl. Med. Biol. 31 (2004) 199–203.
[10] T. Chu, S. Hu, B. Wei, Y. Wang, X. Liu, X. Wang, Bioorg. Med. Chem. Lett. 14 (2004) 747–749.
[11] Y. Zhang, T. Chu, X. Gao, X. Liu, Z. Yang, Z. Guo, X. Wang, Bioorg. Med. Chem. Lett. 16 (2006) 1831–1833.
[12] P. Goldman, J. Antimicrob. Chemother. 10 (Suppl. A) (1982) 23–33.
[13] I.J. Stratford, C. Williamson, C. Hardy, Br. J. Cancer 44 (1981) 109–116.
[14] D.J. Yang, S. Ilgan, T. Higuchi, F. Zareneyrizi, C.S. Oh, C.W. Liu, E.E. Kim, D.A. Podoloff, Pharm. Res. 16 (1999) 743–750.
[15] K.E. Linder, Y.W. Chan, J.E. Cyr, D.P. Nowotnik, W.C. Eckelman, A.D. Nunn, Bioconjug. Chem. 4 (1993) 326–333.
[16] K.E. Linder, Y.W. Chan, J.E. Cyr, M.F. Malley, D.P. Nowotnik, A.D. Nunn, J. Med. Chem. 37 (1994) 9–17.
[17] M. Nakayama, H. Saigo, A. Koda, K. Ozeki, K. Harada, A. Sugii, S. Tomiguchi, A. Kojima, M. Hara, R. Nakashima, Y. Ohyama, M. Takahashi, J. Takata, Y. Karube, Appl. Radiat. Isot. 45 (1994) 735–740.
[18] M. Nakayama, L.C. Xu, Y. Koga, K. Harada, A. Sugii, H. Nakayama, S. Tomiguchi, A. Kojima, Y. Ohyama, M. Takahashi, I. Okabayashi, Appl. Radiat. Isot. 48 (1997) 571–577.
[19] H. Zhu, L. Huang, Y. Zhang, X. Xu, Y. Sun, Y.M. Shen, J. Biol. Inorg. Chem. 15 (2010) 591–599.
[20] J.R. Ballinger, D.S. Cowan, I. Boxen, Z.M. Zhang, A.M. Rauth, J. Nucl. Med. 34 (1993) 242–245.
[21] J.L. Dearling, J.S. Lewis, G.E. Mullen, M.T. Rae, J. Zweit, P.J. Blower, Eur. J. Nucl. Med. 25 (1998) 788–792.
[22] J.R. Ballinger, M.K.J. Wan, A.M. Rauth, J. Nucl. Med. 37 (1996) 1023–1031.
[23] M.A. Varia, D.P. Calkins-Adams, L.H. Rinker, A.S. Kennedy, D.B. Novotny, W.C. Fowler Jr., J.A. Raleigh, Gynecol. Oncol. 71 (1998) 270–277.
[24] J.A. Raleigh, S.C. Chou, G.E. Arteel, M.R. Horsman, Radiat. Res. 151 (1999) 580–589.